Chapter 2
Metal and Alloy Nanoparticles Formed by Laser-Induced Nucleation Method

Takahiro Nakamura

Abstract Tightly focused high-energy femtosecond pulsed laser can create an intense optical field near the focal point. When this intense optical field is formed in the aqueous solution, solvated electrons and radicals are generated by laser-induced photochemical decomposition of water molecules. Due to the strong reducing power of solvated electrons, metal ions in the solution are reduced to form nanoparticles (NPs). In addition, sequential pulsed-laser irradiation causes fragmentation of the formed NPs similar to a scheme of pulsed-laser ablation in liquid, in which the surface of the NPs is negatively charged, resulting in a stable colloidal suspension of NPs without the addition of dispersants. We named this laser-induced physico-chemical NP synthesis method as laser-induced nucleation method. By utilizing this technique, we have succeeded in fabricating not only various noble metal NPs but also solid-solution alloy NPs, which are difficult to fabricate by conventional thermal equilibrium methods due to their immiscible nature. The constituent elements in alloy NPs are the uniformly distributed, and the elemental composition reflects the mixing ratio of the ions in the solution. In this chapter, the reactions in the laser-induced NP formation and some examples for metal and solid-solution alloy NPs produced by the laser-induced nucleation method are introduced.

Keywords Femtosecond laser · Nanoparticles · Solid-solution alloy · Colloidal suspension

2.1 Introduction

Laser processing, which is the application of laser light to materials science, has expanded to not only heating and welding using laser light as a heat source, but also cutting, drilling, surface modification, and marking using ablation reactions, and particle and thin film formation using pulsed-laser ablation (PLA). In addition, it is applying to additive manufacturing, such as powder-bed fusion [1] and laser

T. Nakamura (✉)
Institute of Multidisciplinary Research for Advanced Materials, Tohoku University, Sendai, Miyagi 980-8577, Japan
e-mail: nakamu@tohoku.ac.jp

Y. Ishikawa et al. (eds.), *High-Energy Chemistry and Processing in Liquids*,
https://doi.org/10.1007/978-981-16-7798-4_2

cladding [2]. The laser processing using an unfocused beam needs that the laser wavelength corresponds to absorption band of the material. Meanwhile, a focused beam of high-energy pulsed laser allows to process materials that do not absorb the laser beam by nonlinear optical effects near the focal point. In this case, the laser light source can be selected according to physical properties of the target material and content of the process, because the laser wavelength is free from the absorption of the target material.

Most of laser processing is carried out under atmospheric conditions or in a vacuum, and at the same time, it has recently been reported for a laser processing that utilizes the unique reaction field of a solid material in liquid by irradiating it with laser light. For example, in the pulsed-laser ablation in liquid (PLAL), a pulsed laser beam is focused and irradiated on a solid material immersed or dispersed in a liquid that is transparent to the laser beam. In the PLAL, the energy of the laser beam is absorbed only by the solid material in the liquid, and the resulting ablation reaction produces fine particles "smaller" than the raw material. The formation of various metal nanoparticles (NPs) [3] and organic NPs [4] has been reported. In contrast, in the pulsed-laser melting in liquid (PLML) method [5–8], the aggregates of NPs dispersed in the liquid absorb the energy of the unfocused pulsed laser beam and melt and solidify to produce submicron spherical particles "larger" than the raw material. The submicron spherical particles obtained by this method are relatively uniform in size due to the fact that the average particle size is determined by the energy density of the irradiated laser in relation to the absorption cross section for the laser beam and the heat capacity of the particle [8]. In addition, they have a crystalline structure despite their spherical shape. As described above, the laser processing is widely used in both top-down and bottom-up methods. And in most cases, the laser processing is used to change the shape of the material with maintaining its crystalline structure and properties. Therefore, the laser fluence (energy density, J/cm^2) is controlled to a certain level in order to minimize the heat-affected zone (HAZ) as much as possible in laser cutting and drilling, to suppress the generation of large particles called debris or fragments in particle and thin film formation, or to prevent phase transformation of materials.

On the other hand, with the markedly progress of ultrashort pulse laser technology, current laser is capable of forming unexplored ultra-dense energy fields due to its high peak power characteristics. The irradiation of an ultrashort laser pulse with a very short duration to the target material generates ultra-dense energy field. It induces nonlinear and non-equilibrium reactions, which are different from thermal equilibrium reactions of heat, photolysis, and ionization in conventional laser processes.

We have studied the fabrication of metal and alloy NPs in the high energetic field produced by focused femtosecond laser pulses which is named as "laser-induced nucleation method". In this chapter, we introduce the reactions in laser-induced nucleation method and the fabrication of metal and solid-solution alloy NPs with controlled compositions.

2.2 Formation Mechanism of NPs by Laser-Induced Nucleation Method

For the formation of metal NPs, the chemical reduction in liquid is widely used. In the method, metal ions are reduced to zero-valent atoms by adding a reducing agent into a solution containing various metal ions (nucleation), and the subsequent ripening process (nuclear growth) is controlled by the reaction conditions such as pH and temperature to produce NPs with the desired size and shape. In addition, NPs are usually prepared by adding dispersants to the solution or by coexisting with supporting materials, because NPs are active due to the large specific surface area, and need to be stabilized by coating their surface with dispersants or by fixing them to supporting materials.

On the other hand, it has been reported that Au NPs are formed through photochemical reduction in the strong light field generated by focusing an ultrashort pulsed laser beam into an aqueous solution containing gold ions [9–18]. Formation of Au NPs in the laser-excited field in our study is introduced as an example [10]. Figure 12. shows laser irradiation of an aqueous solution of gold ion (a) just after starting and (b) after 15 min irradiation. An aqueous solution of tetrachloroauric (III) acid trihydrate ($HAuCl_4 \cdot 3H_2O$) with a concentration of 2.5×10^{-4} mol dm^{-3} was held in a synthetic fused silica cuvette. A femtosecond pulsed laser beam with a wavelength of 800 nm, a pulse width of 100 fs, and an average pulse energy of 5.5 mJ was tightly focused through an aspheric lens with a focal length of 8 mm and a numerical aperture of 0.5 for a fixed period of time at a specified repetition rate. Bright plasma was observed near the focal point by the laser irradiation, white light emission through the nonlinear optical effect was confirmed behind the focal point along the direction of laser incidence, and oxygen and hydrogen gas were generated near the focal point (Fig. 2.1a). These phenomena suggest the decomposition of water

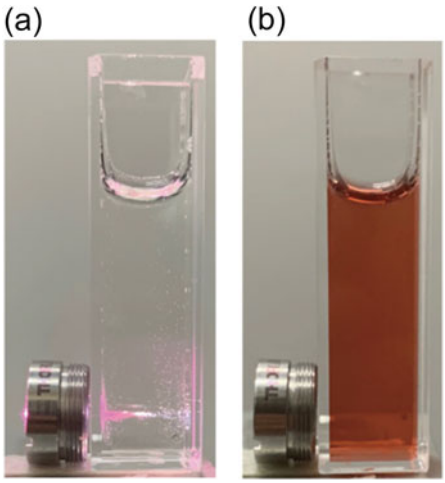

Fig. 2.1 Laser irradiation of an aqueous gold chloride solution **a** just after starting and **b** after 15 min irradiation

molecules by a high-intensity field near the focal point. The aqueous solution, which was colorless and transparent before laser irradiation, turned red after a certain period of laser irradiation (Fig. 2.1b). The UV-visible absorption spectrum of the aqueous solution after laser irradiation showed an absorption peak around 520 nm, which was attributed to the localized surface plasmon resonance (SPR) of the Au NPs. The particles formed in the solution were observed by transmission electron microscopy, and it was confirmed that spherical Au NPs with an average diameter of less than 5 nm were formed.

The formation mechanism of the NPs is presumed to be based on the following reaction [19–24],

$$H_2O\,(nh\nu) \rightarrow e^- + H^+ + OH \tag{2.1}$$

$$e^- \rightarrow e^-_{aq} \tag{2.2}$$

$$H_2O\,(nh\nu) \rightarrow H^{\cdot} + OH^{\cdot} \tag{2.3}$$

$$2OH^{\cdot} \rightarrow H_2O_2 \tag{2.4}$$

$$H^{\cdot} + H_2O \rightarrow H_3O^+ + e^-_{aq} \tag{2.5}$$

$$M^+ + e^-_{aq} \rightarrow M^0 \tag{2.6}$$

$$M^0 \rightarrow M^0_2 \rightarrow \cdots \rightarrow M^0_n \tag{2.7}$$

Nonlinear optical effects such as multiphoton absorption and avalanche photoionization occur, and the energy of the laser light is absorbed by water molecules. In the process, water molecules are decomposed (2.1), and solvated electrons (e^-_{aq}), hydrogen radicals ($H^{\cdot}$), and hydroxyl radicals ($OH^{\cdot}$) are produced (2.2 and 2.3). The hydrogen radicals are consumed on the order of picoseconds (2.5) and are not considered to contribute to the reduction reaction [21]. On the other hand, the redox potential of solvated electrons is $-2.77\ V_{SHE}$, and their lifetime in pure water is several hundred nanoseconds [20]. Therefore, gold ions in aqueous solution are reduced by solvated electrons to zero-valent gold atoms (2.6), which grow to form Au NPs (7). At the same time, the hydroxyl radicals oxidize water to form hydrogen peroxide (2.4). Formation mechanism of Au NPs by the laser-induced method has been intensively studied by Tibbets group [14, 15]. According to their dedicated effort, size and size distribution of Au NPs could be tuned by manipulating the nucleation and growth rate by controlling solution pH and addition of hydroxyl radical scavengers.

The zeta potential of Au NPs prepared under specific conditions was −35 mV (the pH of the aqueous solution is about 3.0), and dispersion state of formed colloidal suspension was stable over several months without the addition of dispersants.

Figure 2.2 shows (a) real-time UV-visible absorption spectra of the colloidal suspension of Au NPs and (b) variation of peak absorbance as a function of irradiation period [25]. The absorption peak originated from SPR of Au NPs increased with irradiation period (Fig. 2.2a), and when the repetition rate of the laser pulse was 100 Hz, the absorption peak reached its maximum in about 14 min (Fig. 2.2b). This is thought to be due to the reduction of all the gold ions in the aqueous solution.

Figure 2.3 shows the UV-visible absorption spectra of the colloidal dispersions in which the laser irradiation was stopped after 9 min, while the gold chloride ions in the aqueous solution were being reduced, and the colloidal dispersions in which the laser irradiation was continued for 20 min after all the gold ions in the solution were reduced. In the colloidal suspension of Au NPs prepared with a short laser irradiation

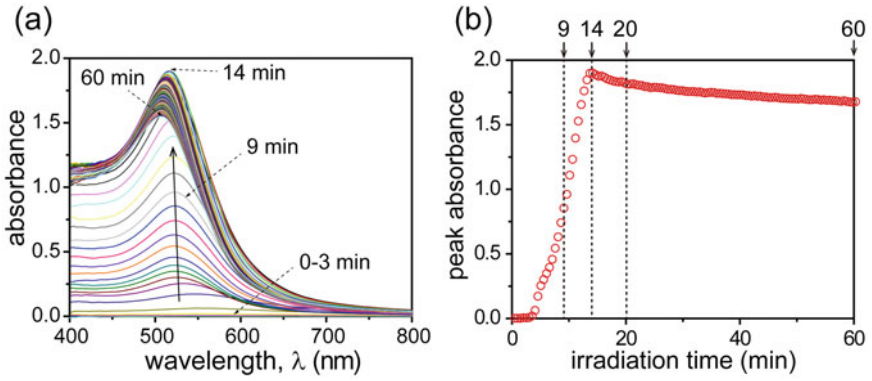

Fig. 2.2 **a** Real-time UV-visible absorption spectra of the colloidal suspension of Au NPs and **b** variation of peak absorbance as a function of irradiation period. Reproduced from Ref. [25] under the terms of the CC-BY 4.0 license. Copyright: (2022) The Authors, published by Hosokawa Powder Technology Foundation

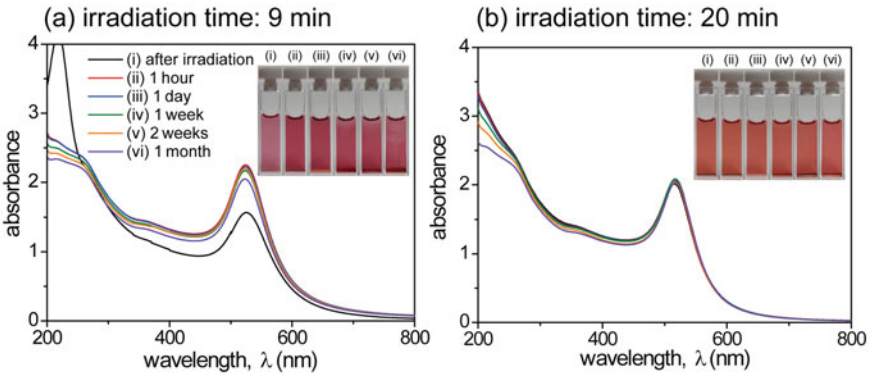

Fig. 2.3 Time evolution of colloidal suspensions of Au NPs prepared by **a** 9 min and **b** 20 min laser irradiation

time (9 min) (Fig. 2.3a), the autocatalytic reaction of the Au NPs formed by the laser irradiation reduced the remaining gold ions in the aqueous solution, causing crystal growth of the formed Au NPs and subsequent aggregation and precipitation. Therefore, the dispersion state of the colloidal suspension was not sustained. On the other hand, in the colloidal Au NPs dispersion (20 min, Fig. 2.3b), which was continuously irradiated even after all the gold chloride ions had been reduced, there was no change in the color and absorption spectrum of the colloidal suspension after one month. This is thought to be due to the fragmentation of the formed NPs by sequential laser irradiation, in a scheme similar to pulsed-laser ablation in liquid (PLAL), and Au NPs are stabilized by bonding with oxygen [26]. According to the study on Au NPs formation by PLAL, the surface state of Au NPs depends on the pH of the solution and is reported to be Au-O^- at pH > 5.8 and Au-OH at pH < 5.8. The pH of the colloidal suspension of Au NPs prepared by the method was approximately 3.0, so the surface structure of the Au NPs was assumed to be Au-OH. The Au NPs prepared in this way can be fixed simply by dropping a colloidal suspension onto a substrate, and it is easy to form composite materials in combination with various carriers while maintaining the excellent surface properties of the NPs. By using this technique, platinum (Pt) [27] and silver (Ag) NPs [28] can be also fabricated.

2.3 Formation of Solid-Solution Alloy Nanoparticles from Mixed Solutions by Laser-Induced Nucleation Method

In the laser-induced nucleation method, since the target of laser irradiation is an aqueous solution, it is easy to form alloy NPs by laser irradiation of aqueous solutions containing multiple metallic ions. As mentioned above, we have successfully prepared colloidal suspension of Au and Ag NPs by the method. The synthesis of these NPs involved aqueous solutions prepared by dissolving gold (III) chloride trihydrate ($HAuCl_4 \cdot 3H_2O$) or silver (I) nitrate ($AgNO_3$, both from Fujifilm Wako Pure Chemicals) in ultrapure water (18.2 MΩ, arium® pro UV, Sartorius). When these solutions were mixed, silver chloride (AgCl) insoluble in water was produced above a certain ionic concentration. Therefore, to prepare a mixed aqueous solution, we separately prepared each aqueous solution of metal ions with a concentration of 2.5×10^{-4} mol dm^{-3}, added 0.1 vol% ammonia water to them, and then mixed them with desired molar concentration of metal ions in each prepared aqueous solution to suppress the formation of silver chloride. Figure 2.4 shows the colloidal suspension of NPs prepared by laser irradiation of mixed aqueous solutions of Au and Ag ions with different mixing ratios and corresponding UV-visible absorption spectra of the colloidal suspensions. The aqueous solutions before laser irradiation were colorless and transparent in all cases, but the colloidal suspensions after laser irradiation showed a systematic change from yellow to reddish purple depending on the mixing ratio of metallic ions (Fig. 2.4a). The absorption spectra of the colloidal suspensions

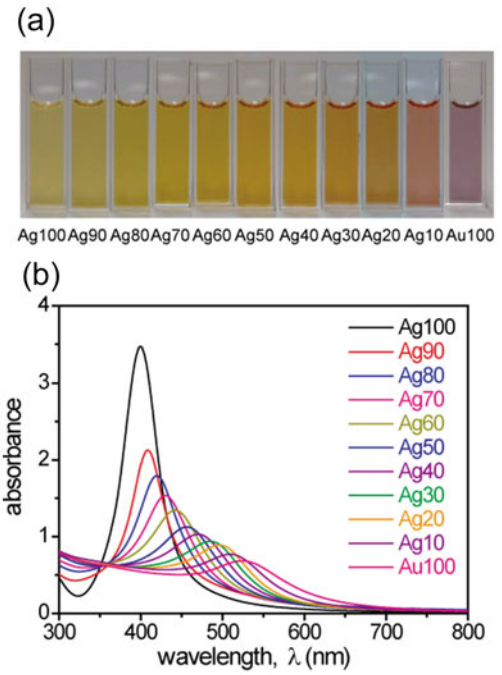

Fig. 2.4 **a** Colloidal suspensions prepared by laser irradiation of mixed aqueous solutions of Au and Ag ions with different mixing ratios, **b** corresponding UV-visible absorption spectra

of Ag and Au NPs showed absorption peaks of SPR near 400 and 520 nm, respectively, while those shifted to the longer wavelength side as the molar ratio of gold ions in the mixture increased (Fig. 2.4b). The absorption peak positions in the spectra as a function of the molar ratio of Au in the aqueous solutions are shown in Fig. 2.5. The absorption peak position in the absorption spectrum showed a proportional relationship to the molar ratio of Au in the aqueous solution, suggesting the formation of composition-controlled Au-Ag alloy NPs by laser irradiation of mixture solutions.

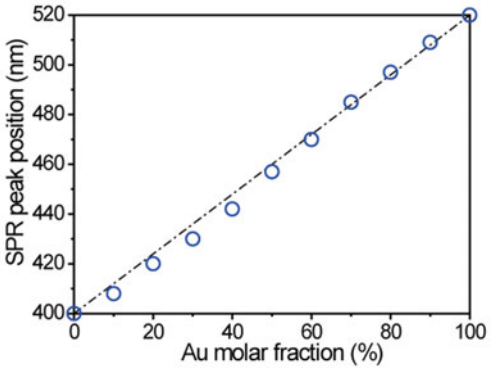

Fig. 2.5 Relationship between SPR peak positions in the absorption spectra and the molar ratio of Au in the mixed aqueous solutions

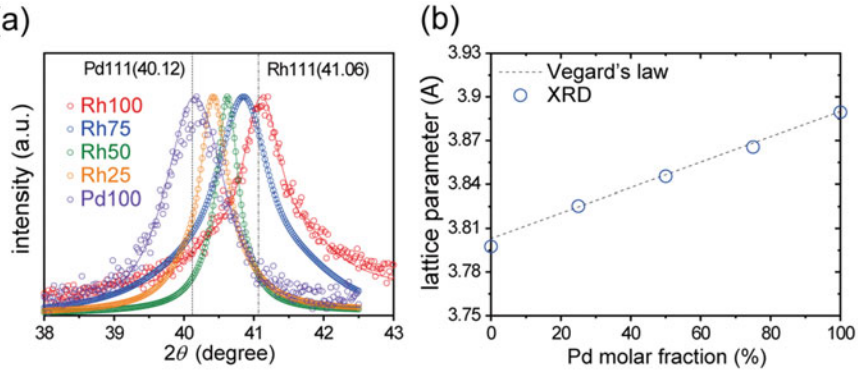

Fig. 2.6 Relationship between **a** X-ray diffraction patterns of alloy NPs prepared by laser irradiation of mixed aqueous solutions of Rh and Pd ions and **b** lattice constants determined from X-ray peak positions and the molar ratio of Pd in the mixed aqueous solutions

Since Au and Ag have redox potentials of +0.93 V_{SHE} and +0.7996 V_{SHE}, respectively, co-reduction with a relatively strong reducing agent is necessary to produce Au-Ag alloy NPs by chemical reduction. The formation of Au-Ag alloy NPs in the laser-induced nucleation method can be attributed to the high reducing power of the hydrated electrons described above.

While Au-Ag binary alloys are considered to be easy to form in terms of thermal energy because they form solid-solution alloy in bulk, the laser-induced nucleation method can also produce non-equilibrium alloy NPs which are difficult to fabricate by conventional methods [29–34]. As an example, we show the formation of rhodium (Rh)–palladium (Pd) binary alloy NPs. Rhodium (III) chloride trihydrate ($RhCl_3 \cdot 3H_2O$) and palladium (II) chloride ($PdCl_2$, both from Fujifilm Wako Pure Chemicals) were dissolved in extra pure water to prepare aqueous solutions with a concentration of 2.5×10^{-4} mol dm^{-3}. The laser irradiation was performed on the mixed aqueous solutions. Figure 2.6 shows the results of X-ray diffraction measurements of the fabricated NPs and the relationship between the molar ratio of Pd in the solution and the interplanar spacings determined from the peak positions. The X-ray diffraction peak exhibited a single Gaussian pattern characteristic of the face-centered cubic structure, and the peak positions were systematically shifted according to the metal ion mixing ratio in the aqueous solution. The interplanar spacings of the NPs calculated from the positions of the X-ray diffraction peaks and the mixing ratio of metallic ion in the aqueous solution were proportional according to the Vegard's law, indicating the formation of Rh-Pd alloy NPs with a tunable composition. In addition, elemental mapping of the alloy NPs obtained by scanning transmission electron microscopy–energy dispersive X-ray analysis (STEM–EDS) (Fig. 2.7) showed that rhodium and palladium are uniformly distributed in the particles, confirming the formation of solid-solution alloy NPs. Because of the wide immiscibility gap in the Rh-Pd binary phase diagram, solid-solution alloy NPs are difficult to fabricate in thermal equilibrium. The laser-induced nucleation method allows the co-reduction

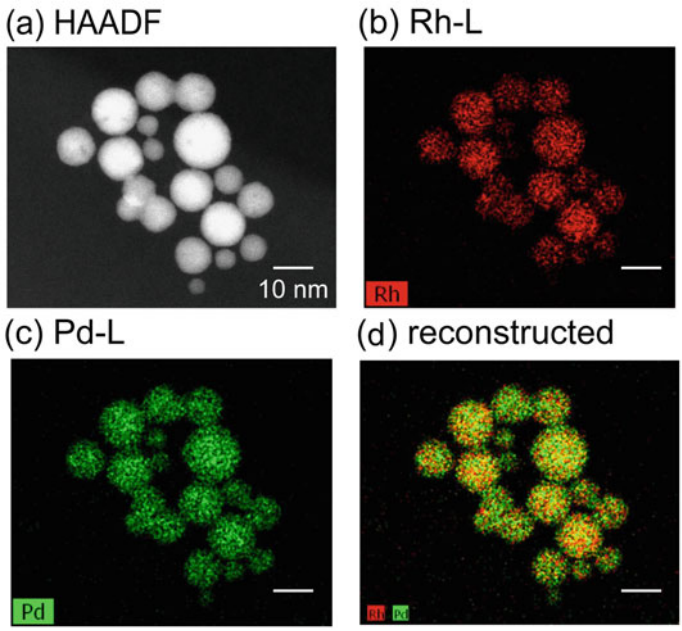

Fig. 2.7 STEM-EDS mappings of alloy NPs prepared by laser irradiation of Rh and Pd mixed aqueous solutions. **a** HAADF-STEM image, two-dimensional mapping image of **b** Rh and **c** Pd, and **d** superimposed two-dimensional image of Rh and Pd

of multiple ions by radicals with strong reducing power. In addition, it also induces the non-equilibrium reactions, where the reduction occurs repeatedly in a very short time during the radical lifetime formed by each irradiated laser pulse. As the result of this, an alloy structure was formed before the atoms diffuse in thermal equilibrium condition. This is different from conventional chemical reduction or reduction by radicals caused by continuous high-energy irradiation such as electron beams or gamma rays.

2.4 Summary

In this chapter, we report on the fabrication of multigrid all-solid-solution alloy NPs by a laser-induced nucleation method using an intense reaction field created by ultrashort laser pulses and the reaction field as a novel physicochemical nanoparticle synthesis method. The works showed that this method enables us to control the composition of alloys with combinations that are normally difficult to fabricate in the full rate solid-solution state. We are currently working on the construction of a mass synthesis system and the preparation of surface-modified nanoparticle colloids,

which are stable in water and modified with desired modifiers, for a wide range of applications of the prepared NPs.

Acknowledgements The author thanks Mr. Yuichiro Hayasaka for his help with STEM-EDS analysis.

References

1. B.P. Conner, G.P. Manogharan, A.N. Martof, L.M. Rodomsky, C.M. Rodomsky, D.C. Jordan, J.W. Limperos, Making sense of 3-D printing: Creating a map of additive manufacturing products and services. Addit. Manuf. **1–4**, 64–76 (2014). https://doi.org/10.1016/j.addma.2014.08.005
2. Y. Sato, M. Tsukamoto, T. Shobu, Y. Funada, Y. Yamashita, T. Hara, M. Sengoku, Y. Sakon, T. Ohkubo, M. Yoshida, N. Abe, In situ X-ray observations of pure-copper layer formation with blue direct diode lasers. Appl. Phys. Sci. **480**, 861–867 (2019). https://doi.org/10.1016/j.apsusc.2019.03.057
3. Z. Yan, D.B. Chrisey, Pulsed laser ablation in liquid for micro-/nanostructure generation. J. Photochem. Photobiol. C: Photochem. Rev. **13**, 204–223 (2012). https://doi.org/10.1016/j.jphotochemrev.2012.04.004
4. R. Yanagihara, T. Asahi, Y. Ishibashi, O. Odawara, H. Wada, Fabrication of naphthalocyanine nanoparticles by laser ablation in liquid and application to contrast agents for photoacoustic imaging. Jpn. J. Appl. Phys. **57**(2018). https://doi.org/10.7567/JJAP.57.035001
5. Y. Ishikawa, Q. Feng, N. Koshizaki, Growth fusion of submicron spherical boron carbide particles by repetitive pulsed laser irradiation in liquid media. Appl. Phys. A **99**, 797–803 (2010). https://doi.org/10.1007/s00339-010-5745-6
6. Y. Ishikawa, T. Sasaki, N. Koshizaki, Submicron-sized boron carbide particles encapsulated in turbostratic graphite prepared by laser fragmentation in liquid medium. J. Nanosci. Nanotechnol. **10**, 5467–5470 (2010). https://doi.org/10.1166/jnn.2010.1947
7. H.Q. Wang, A. Pyatenko, K. Kawaguchi, X. Li, Z. Swiatkowska-Warkocka, N. Koshizaki, Selective pulsed heating for the synthesis of semiconductor and metal submicrometer spheres. Angew. Chem. Int. Ed. **49**, 6361–6364 (2010). https://doi.org/10.1002/anie.201002963
8. A. Pyatenko, H. Wang, N. Koshizaki, Growth mechanism of monodisperse spherical particles under nanosecond pulsed laser irradiation. J. Phys. Chem. C **118**, 4495–4500 (2014). https://doi.org/10.1021/jp411958v
9. C. Zhao, S. Qu, J. Qiu, C. Zhu, Photoinduced formation of colloidal Au by a nearinfrared femtosecond laser. J. Mater. Res. **18**, 1710–1714 (2003). https://doi.org/10.1557/JMR.2003.0235
10. T. Nakamura, Y. Mochidzuki, S. Sato, Fabrication of gold nanoparticles in intense optical field by femtosecond laser irradiation of aqueous solution. J. Mater. Res. **23**, 968–974 (2008). https://doi.org/10.1557/jmr.2008.0115
11. B. Tangeysh, K.M. Tibbetts, J.H. Odhner, B.B. Wayland, R.J. Levis, Gold nanoparticle synthesis using spatially and temporally shaped femtosecond laser pulses: Post-irradiation auto-reduction of aqueous $[AuCl_4]^-$. J. Phys. Chem. C **117**, 18719–18727 (2013). https://doi.org/10.1021/jp4056494
12. J.H. Odhner, K.M. Tibbetts, B. Tangeysh, B.B. Wayland, R.J. Levis, Mechanism of improved Au nanoparticle size distributions using simultaneous spatial and temporal focusing for femtosecond laser irradiation of aqueous $KAuCl_4$. J. Phys. Chem. C **118**, 23986–23995 (2014). https://doi.org/10.1021/jp507873n
13. N. Nakashima, K. Yamanaka, M. Saeki, H. Ohba, S. Taniguchi, T. Yatsuhashi, Metal ion reductions by femtosecond laser pulses with micro-joule energy and their efficiencies. J. Photochem. Photobiol. A **319–320**, 70–77 (2016). https://doi.org/10.1016/J.JPHOTOCHEM.2015.12.021

14. K.M. Tibbetts, B. Tangeysh, J.H. Odhner, R.J. Levis, Elucidating strong field photochemical reduction mechanisms of aqueous $[AuCl_4]^-$: Kinetics of multiphoton photolysis and radical-mediated reduction. J. Phys. Chem. A **120**, 3562–3569 (2016). https://doi.org/10.1021/acs.jpca.6b03163
15. V.K. Meader, M.G. John, C.J. Rodrigues, K.M. Tibbetts, Roles of free electrons and H_2O_2 in the optical breakdown-induced photochemical reduction of aqueous $[AuCl_4]^-$. J. Phys. Chem. A **121**, 6742−6754 (2017). https://doi.org/10.1021/acs.jpca.7b05370
16. C.J. Rodrigues, J.A. Bobb, M.G. John, S.P. Fisenko, M.S. El-Shall, K.M. Tibbetts, Nucleation and growth of gold nanoparticles initiated by nanosecond and femtosecond laser irradiation of aqueous $[AuCl_4]^-$. Phys. Chem. Chem. Phys. **20**, 28465–28475 (2018). https://doi.org/10.1039/C8CP05774E
17. H. Belmouaddine, M. Shi, P.-L. Karsenti, R. Meesat, L. Sanche, D. Houde, Dense ionization and subsequent non-homogeneous radical-mediated chemistry of femtosecond laser-induced low density plasma in aqueous solutions: Synthesis of colloidal gold. Phys. Chem. Chem. Phys. **19**, 7897–7909 (2017). https://doi.org/10.1039/C6CP08080D
18. H. Belmouaddine, M. Shi, L. Sanche, D. Houde, Tuning the size of gold nanoparticles produced by multiple filamentation of femtosecond laser pulses in aqueous solutions. Phys. Chem. Chem. Phys. **20**, 23403–23413 (2018). https://doi.org/10.1039/C8CP02054J
19. K. Kurihara, J. Kizling, P. Stenius, J.H. Fendler, Laser and pulse radiolytically induced colloidal gold formation in water and in water-in-oil microemulsions. J. Am. Chem. Soc. **105**, 2574–2579 (1983). https://doi.org/10.1021/ja00347a011
20. D.N. Nikogosyan, A.A. Oraevsky, V.I. Rupasov, Two-photon ionization and dissociation of liquid water by powerful laser UV radiation. Chem. Phys. **77**, 131–143 (1983). https://doi.org/10.1016/0301-0104(83)85070-8
21. R.A. Crowell, D.M. Bartels, Multiphoton ionization of liquid water with 3.0−5.0 eV photons. J. Phys. Chem. **100**, 17940−17949 (1996). https://doi.org/10.1021/jp9610978
22. A. Reuther, A. Laubereau, D.N. Nikogosyan, Primary photochemical processes in water. J. Phys. Chem. **100**, 16794–16800 (1996). https://doi.org/10.1021/jp961462v
23. S.L. Chin, S. Lagace, Generation of H_2, O_2, and H_2O_2 from water by the use of intense femtosecond laser pulses and the possibility of laser sterilization. Appl. Opt. **35**, 907–911 (1996). https://doi.org/10.1364/AO.35.000907
24. S. Pommeret, F. Gobert, M. Mostafavi, I. Lampre, J.-C. Mialocq, Femtochemistry of the hydrated electron at decimolar concentration. J. Phys. Chem. A **105**, 11400–11406 (2001). https://doi.org/10.1021/jp0123381
25. T. Nakamura, Y. Yamazaki, S. Sato, Synthesis of noble metals and their alloy nanoparticles by laser-induced nucleation in a highly intense laser field (2020). https://doi.org/10.14356/kona.2022002
26. J.-P. Sylvestre, S. Poulin, A. Kabashin, E. Sacher, M. Meunier, J.H.T. Luong, Surface chemistry of gold nanoparticles produced by laser ablation in aqueous media. J. Phys. Chem. B **108**, 16864–16869 (2004). https://doi.org/10.1021/jp047134+
27. T. Nakamura, K. Takasaki, A. Ito, S. Sato, Fabrication of platinum particles by intense, femtosecond laser pulse irradiation of aqueous solution. Appl. Surf. Sci. **255**, 9630–9633 (2009). https://doi.org/10.1016/j.apsusc.2009.04.092
28. T. Nakamura, H. Magara, Y. Herbani, S. Sato, Fabrication of silver nanoparticles by highly intense laser irradiation of aqueous solution. Appl. Phys. A **104**, 1021 (2011). https://doi.org/10.1007/s00339-011-6499-5
29. Y. Herbani, T. Nakamura, S. Sato, Synthesis of platinum-based binary and ternary alloy nanoparticles in an intense laser field. J. Coll. Int. Sci. **375**, 78–87 (2012). https://doi.org/10.1016/j.jcis.2012.02.030
30. T. Nakamura, Y. Herbani, S. Sato, Fabrication of solid-solution gold–platinum nanoparticles with controllable compositions by high-intensity laser irradiation of solution. J. Nanopart. Res **14**, 785 (2012). https://doi.org/10.1007/s11051-012-0785-9

31. M.S.I. Sarker, T. Nakamura, Y. Herbani, S. Sato, Fabrication of Rh based solid-solution bimetallic alloy nanoparticles with fully-tunable composition through femtosecond laser irradiation in aqueous solution. Appl. Phys. A **110**, 145–152 (2013). https://doi.org/10.1007/s00339-012-7467-4
32. M.S.I. Sarker, T. Nakamura, S. Sato, Composition-controlled ternary Rh–Pd–Pt solid-solution alloy nanoparticles by laser irradiation of mixed solution of metallic ions. J. Mater. Res. **29**, 856–864 (2014). https://doi.org/10.1557/jmr.2014.62
33. M.S.I. Sarker, T. Nakamura, S. Sato, All-proportional solid-solution Rh–Pd–Pt alloy nanoparticles by femtosecond laser irradiation of aqueous solution with surfactant. J. Nanopart. Res. **17**, 259 (2015). https://doi.org/10.1007/s11051-015-3056-8
34. M.S.I. Sarker, T. Nakamura, S. Kameoka, Y. Hayasaka, S. Sato, Enhanced catalytic activity of inhomogeneous Rh-based solid-solution alloy nanoparticles. RSC Adv. **9**, 38882–38890 (2019). https://doi.org/10.1039/C9RA06167C